# $\alpha$ Decay of $^{109}$I and Its Implications for the Proton Decay of $^{105}$Sb and the Astrophysical Rapid Proton-Capture Process

C. Mazzocchi,[1,2] R. Grzywacz,[1,3] S. N. Liddick,[4] K. P. Rykaczewski,[3] H. Schatz,[5] J. C. Batchelder,[4] C. R. Bingham,[1,3] C. J. Gross,[3] J. H. Hamilton,[6] J. K. Hwang,[6] S. Ilyushkin,[7] A. Korgul,[1,6,8,9] W. Królas,[9,10] K. Li,[6] R. D. Page,[11] D. Simpson,[1,12] and J. A. Winger[4,7,9]

[1]Department of Physics and Astronomy, University of Tennessee, Knoxville, Tennessee 37996, USA
[2]IFGA, University of Milan and INFN, Milano, I-20133, Italy
[3]Physics Division, Oak Ridge National Laboratory, Oak Ridge, Tennessee 37831, USA
[4]UNIRIB, Oak Ridge Associated Universities, Oak Ridge, Tennessee 37831, USA
[5]National Superconducting Cyclotron Laboratory, Michigan State University, East Lansing, Michigan 48824, USA
[6]Department of Physics and Astronomy, Vanderbilt University, Nashville, Tennessee 37235, USA
[7]Department of Physics and Astronomy, Mississippi State University, Mississippi 39762, USA
[8]Institute of Experimental Physics, Warsaw University, Warszawa, PL 00-681, Poland
[9]Joint Institute for Heavy-Ion Reactions, Oak Ridge, Tennessee 37831, USA
[10]Institute of Nuclear Physics, Polish Academy of Sciences, PL 31-342 Kraków, Poland
[11]Department of Physics, University of Liverpool, Liverpool, L69 7ZE, United Kingdom
[12]Department of Physics, Astronomy, and Geology, East Tennessee State University, Johnson City, Tennessee 37614, USA

(Received 7 March 2007; published 23 May 2007)

An $\alpha$-decay branch of $(1.4 \pm 0.4) \times 10^{-4}$ has been discovered in the decay of $^{109}$I, which predominantly decays via proton emission. The measured $Q_\alpha$ value of $3918 \pm 21$ keV allows the indirect determination of the $Q$ value for proton emission from $^{105}$Sb of $356 \pm 22$ keV, which is approximately of 130 keV more bound than previously reported. This result is relevant for the astrophysical rapid proton-capture process, which would terminate in the $^{105}$Sn$(p,\gamma)^{106}$Sb$(p,\gamma)^{107}$Te($\alpha$ decay)$^{103}$Sn cycle at the densities expected in explosive hydrogen burning scenarios, unless unusually strong pairing effects result in a $^{103}$Sn$(p,\gamma)^{104}$Sb$(p,\gamma)^{105}$Te($\alpha$ decay)$^{101}$Sn) cycle.

DOI: 10.1103/PhysRevLett.98.212501 PACS numbers: 23.60.+e, 21.10.Dr, 23.50.+z, 27.60.+j

Experimentally delineating the limits of bound nuclei is one of the major challenges for modern nuclear physics. It tests the quality of theoretical model predictions for one of the fundamental properties of the atomic nucleus, its binding energy, in the extreme situation where it becomes unstable against nucleon emission. More than a century after the discovery of $\alpha$ decay [1] and over 35 years after the first observation of direct proton emission [2], measuring the energy released by nuclei undergoing these decay modes still provides a very sensitive and precise method to determine the gradient of the nuclear binding energy surface. The measurement of the emitted particle's energy ($E_\alpha$ or $E_p$), corrected for the recoil effect, yields the difference in binding energy (mass) between the parent and daughter nuclides ($Q_\alpha$ or $Q_p$). This is especially important at the farthest extremes from the valley of $\beta$ stability, where any measurement of nuclear properties is extremely difficult. Indeed, particle-decay spectroscopy exploiting efficient separation devices is often the only way to measure separation energies for these short-lived nuclei with high precision ($\sim 10$ keV) from the observation of just a few ions. Moreover, these decay modes can be used to probe the wave functions of the nuclear levels involved and to study nuclear shell effects [3–5]. The determination of the nuclear binding energy is extremely important for astrophysically relevant nuclei, since the reaction energies used to model the nucleosynthesis processes are deduced from nuclear masses.

Of particular interest are the nuclei above the doubly magic nucleus $^{100}$Sn, which form an island of $\alpha$ and proton emission. This island's existence directly reflects the strong double shell closure $N = Z = 50$ and the presence of the proton dripline. The odd-$Z$ isotopes in this region are especially fascinating as both $\alpha$ and proton decay may occur. To date, $\alpha$ decay has been observed in $^{108,110-113}$I [6,7] and $^{114}$Cs [8], while their neighboring nuclei $^{109}$I [9] and $^{112,113}$Cs [9,10] are proton emitters. The nuclide $^{105}$Sb was also reported to be a proton emitter [11], but despite many attempts applying various techniques [12–17] the result for $^{105}$Sb [11] has not been confirmed directly. Even so, the deduced binding energy was included in widely used mass tables [18].

An alternative approach to verify the $^{105}$Sb result is to measure the expected small $\alpha$-decay branch of $^{109}$I, which is predominantly a proton emitter having a half-life of $100 \pm 5$ $\mu$s [9,19]. A measurement of the $^{109}$I $\alpha$-decay energy would allow an indirect and independent determination of the proton separation energy ($S_p = -Q_p$) in $^{105}$Sb, since $Q_\alpha(^{109}\mathrm{I}) + Q_p(^{105}\mathrm{Sb}) = Q_p(^{109}\mathrm{I}) + Q_\alpha(^{108}\mathrm{Te})$. However, several attempts to identify this decay could only set upper limits on the $\alpha$-decay branching ratio, $b_\alpha$ (10% if $E_\alpha = 3.7$ MeV and 0.7% if $E_\alpha = 4.3$ MeV [17]; 0.5% [6];

 

0.03% [20] ), proving that the quest for the elusive $\alpha$-decay branch is indeed a challenge.

The $S_p$ value for $^{105}$Sb is of interest for the astrophysical rapid proton-capture ($rp$-) process. This is a reaction sequence of mainly proton captures and $\beta$ decays near the proton dripline that burns hydrogen at extreme temperatures and densities [21,22]. Explosive hydrogen burning via the $rp$ process powers the frequently observed type I (thermonuclear) x-ray bursts. Models suggest that a Sn-Sb-Te cycle is reached in a subset of type I x-ray bursts that burn particularly large amounts of hydrogen, e.g., the first burst after a period of quiescence [23].

Figure 1 shows the reaction sequence in the tin region. A critical question is the amount of material that is processed in the Sn-Sb-Te cycle, as it produces helium at late times in the burst. This enhances the production of seed nuclei for the $rp$ process via the 3-$\alpha$ reaction and could lead to a late boost in energy production, potentially shaping the light curve and affecting the composition of the burst ashes. Current calculations predict that the cycle forms at $^{105}$Sn, as at that point the antimony isotopes become bound enough for proton captures to proceed via $^{105}\mathrm{Sn}(p,\gamma)^{106}\mathrm{Sb}(p,\gamma)^{107}\mathrm{Te}$. A strong $(\gamma,\alpha)$ branch closes the cycle. The $Q_p$ values of the antimony isotopes are critical as they determine at which point along the tin isotopic chain proton captures can proceed towards tellurium and form a cycle. They also determine how many of the relatively long-lived $\beta$ decays beyond $^{103}$Sn have to be overcome before the cycle can be formed. As the Sn-Sb-Te cycle occurs at the very end of the burst, an early onset of the cycle can strongly enhance its influence, while a late onset might only lead to weak or even negligible cycling.

In this Letter we report the discovery of a minuscule $\alpha$-decay branch from $^{109}$I and its consequences for the $S_p$ in $^{105}$Sb and the termination of the $rp$ process.

The $^{109}$I nuclei were produced at the HRIBF at Oak Ridge National Laboratory in the $p2n$ fusion-evaporation channel of the $^{54}\mathrm{Fe} + {}^{58}\mathrm{Ni}$ reaction at 207 MeV. The $^{58}$Ni target was 300 $\mu$g/cm$^2$ thick and isotopically enriched to more than 99%. The recoiling evaporation residues were separated according to their mass-to-charge ratio ($A/Q$) by the Recoil Mass Spectrometer (RMS) [25]. Recoils with $A/Q = 109/27$ and 109/28 were transported to the focal plane of the RMS. After passing through a microchannel plate detector [26] and a 150 $\mu$g/cm$^2$ aluminum degrader, they were implanted into a 67 $\mu$m thick double-sided silicon strip detector (DSSD). The DSSD was surrounded upstream by a SiBox to veto escaping $\alpha$ particles and protons, while a 3.9 mm-thick SiLi detector was placed behind the DSSD to veto $\beta$ particles and $\beta$-delayed protons [27]. The preamplifier signals from each of the DSSD strips ($40 \times 40$) and from the ancillary detectors were read out through a digital signal processing acquisition system [28]. The ion implantation and decay events were correlated in space and time, with a minimum time between an implanted ion and a decay of 20 $\mu$s. Each strip was calibrated using the known energies of the $\alpha$-decay lines of the longer-lived nuclides $^{109}$Te and $^{108}$Te, daughter of $^{109}$I proton emission.

In Fig. 2 a portion of the $\alpha$ energy spectrum between 20 and 400 $\mu$s following an implanted ion is displayed. The peaks at 3107 and 3317 keV correspond to the $\alpha$ decays of $^{109}$Te and $^{108}$Te, respectively. The third peak in the upper-panel spectrum at an energy of $3774 \pm 20$ keV is assigned to the $\alpha$ decay of $^{109}$I. The $^{109}$I $\alpha$-decay energy gives a $Q_\alpha$ value of $3918 \pm 21$ keV.

The assignment is based on the following considerations: no known $\alpha$ emitter in the $^{100}$Sn region has this decay energy; $A/Q$ for the implanted ions is 109/27 or 109/28 and the charge state contaminants ($A/Q = 105/26$ or 105/27) are either more exotic or do not undergo $\alpha$

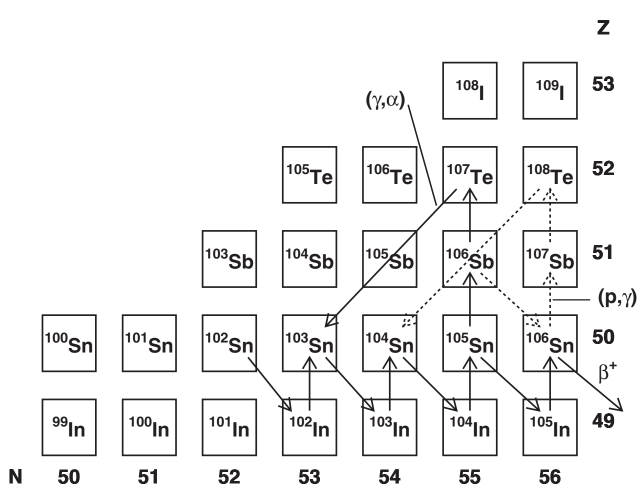


FIG. 1. Portion of the Segrè chart with the path followed by the $rp$ process in the $^{100}$Sn region as predicted in Ref. [24]. See text for details.

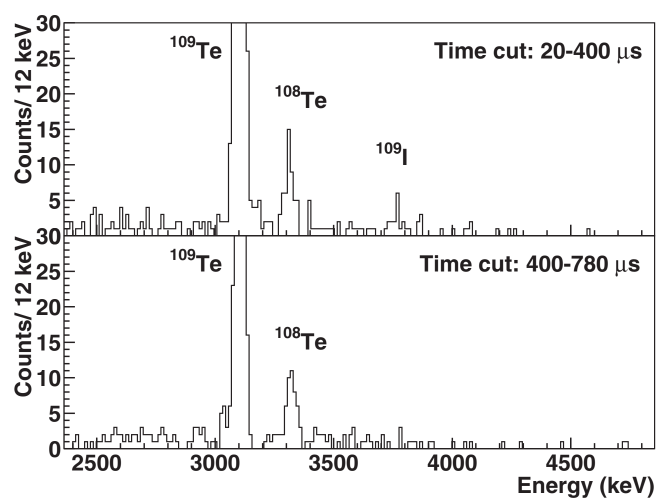


FIG. 2. Portion of the energy spectrum of decay events following implantation of an ion between 20 and 400 $\mu$s (upper panel) and in the 400–780 $\mu$s time interval (lower panel). The peaks are labeled with their precursor. The spectra are vetoed by the SiBox and SiLi detector signals to suppress escape signals and $\beta$ particles and $\beta$-delayed protons.

decay; the time distribution of the events in the 3774 keV transition is compatible with the 100 $\mu$s half-life of $^{109}$I. The possibility that this peak is a random fluctuation in the background can be safely excluded since a statistical analysis indicates likelihood of $2.5 \times 10^{-4}$ for this scenario. With a narrow setting of focal plane collimators, we observed no evidence of neighboring $A = 108, 110$ contamination in our spectra. Moreover, the lower-panel spectrum of Fig. 2 shows decay events in the following 400 to 780 $\mu$s: the 3774 keV peak does not appear.

The branching ratio for the $\alpha$ decay of $^{109}$I can be calculated from the number of $\alpha$ decay events observed, the number of implanted $^{109}$I ions, and the detection efficiency. The intensity of the transition is $16 \pm 4$ counts after correcting the observed $\alpha$-line intensity for the small background and for the dead time of 20 $\mu$s following the ion implantation. The number of implanted $^{109}$I ions is $(1.53 \pm 0.15) \times 10^5$, deduced from the observed $\alpha$ decays of the daughter $^{108}$Te ($70\,370 \pm 270$). This results in $b_\alpha(^{109}\mathrm{I}) = (1.4 \pm 0.4) \times 10^{-4}$. A similar value is deduced from the measured $^{109}$I proton yield but with larger uncertainty due high energy thresholds and dead time effects at short implantation-decay time correlations. The time analysis of the $\sim$112 500 proton events from the decay of $^{109}$I yielded a more precise measurement of the half-life, $T_{1/2} = 93.5 \pm 0.3$ $\mu$s. The partial $\alpha$-decay half-life of $^{109}$I is therefore $0.7 \pm 0.2$ s. The small reduced $\alpha$-decay width relative to $^{212}$Po ($W_\alpha$) [5] is $W_\alpha = (1.9 \pm 0.8) \times 10^{-3}$, which is similar to the value of $(2.9 \pm 0.6) \times 10^{-3}$ deduced for the neighboring odd-A iodine isotope $^{111}$I.

In Fig. 3 the $Q_\alpha$ and $Q_p$ values for the odd-$Z$ $\alpha$ and proton emitters in the $^{100}$Sn region are plotted. The $Q_\alpha = 3918$ keV for $^{109}\mathrm{I}_{56}$ is in good agreement with the systematic trend for the heavier iodine isotopes. The measurement of the $\alpha$-decay energy of $^{109}\mathrm{I}_{56}$ allows an indirect measurement of the $Q_p$ value of $^{105}\mathrm{Sb}_{54}$. Using $Q_p(^{109}\mathrm{I}_{56}) = 828.9 \pm 4.0$ keV [29], $Q_\alpha(^{108}\mathrm{Te}_{56}) = 3445 \pm 4$ keV [30], and our $Q_\alpha(^{109}\mathrm{I}_{56})$ we obtain $Q_p(^{105}\mathrm{Sb}_{54}) = 356 \pm 22$ keV. This corresponds to a partial proton half-life $T^p_{1/2} = 4 \times 10^6$ s and branching ratio $b_p = 3 \times 10^{-7}$ as calculated using the WKB approximation assuming a spherical potential barrier and $l = 2$ emission from a $\pi d_{5/2}$ orbital. It rules out the possibility of observing direct ground-state proton emission from this nucleus, which is more proton bound than previously claimed [11]. The new $Q_p$ value of $^{105}$Sb is in clear disagreement with that of $491 \pm 15$ keV [29] based on $E_p = 478 \pm 15$ keV reported by Tighe *et al.* [11], corresponding to $T^p_{1/2} = 34$ s and $b_p = 3 \times 10^{-2}$. However, both $Q_p$ and $b_p$ are in agreement with the nonobservation and respective limits set by other experiments hunting for this decay branch of $^{105}$Sb over the past 20 years [12–14,17]. This new $Q_p$ value allows one to deduce the mass excess ($\Delta$) for $^{105}$Sb based on the known $\Delta(^{104}\mathrm{Sn})$ [31]: $\Delta(^{105}\mathrm{Sb}) = -63\,925 \pm 131$ keV.

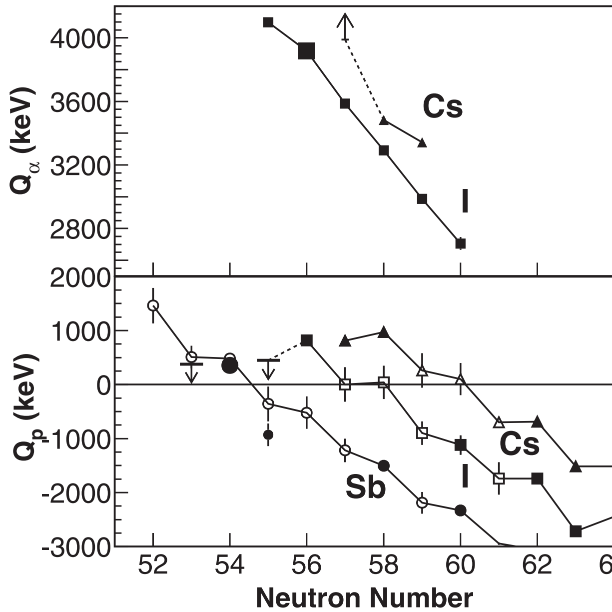


FIG. 3. $Q$ values for $\alpha$ (upper panel) and proton (lower panel) emission, for proton rich odd-$Z$ nuclides in the $^{100}$Sn region. The isotopic chains (Sb circles, I squares, and Cs triangles) are connected with lines. The data for $Q_\alpha(^{109}\mathrm{I}_{56})$ and $Q_p(^{105}\mathrm{Sb}_{54})$, depicted with larger symbols, stem from this work, while the others are taken from literature [6,8,10,18,29,32,33]. In the lower panel full symbols correspond to experimental values, while open symbols are extrapolations [18]. Arrows indicate the upper or lower limit for the respective $Q$ value estimated in this work. The points for $N = 55$ $^{106}$Sb are discussed in the text.

Pairing effects are responsible for the decrease in $Q_p$ value for the odd-odd $^{108}\mathrm{I}_{55}$ and $^{112}\mathrm{Cs}_{57}$ with respect to the odd-even $^{109}\mathrm{I}_{56}$ and $^{113}\mathrm{Cs}_{58}$, respectively, see lower panel of Fig. 3. We expect a similar effect to be present for the antimony isotopes so that we can expect $Q_p(^{104}\mathrm{Sb}_{53}) <$ 378 keV. If the $Q_p$-value systematics for antimony isotopes maintain the same slope as the iodine and cesium isotopes, a $Q_p$ around 0 or even negative can be expected, raising the possibility that $^{104}$Sb is proton bound. More measurements in this direction are needed, not only to understand better the $S_p$ and $\Delta$ of $^{104}$Sb, but also to better understand the effects of pairing on $Q_p$ values. The upper limit for $Q_p(^{104}\mathrm{Sb}_{53})$ implies an upper limit for $Q_p(^{108}\mathrm{I}_{55})$ of 474 keV, see Fig. 3.

In order to explore the impact of the new $Q_p$ value for $^{105}$Sb and the new constraints for $^{104}$Sb on the $rp$ process, we performed reaction network calculations using a one-zone x-ray burst model [24]. This approximation predicts light curves and the final composition of the burst ashes that agree reasonably well with fully one-dimensional models as long as the ignition conditions are comparable. The ignition model used here [24] is adequate for the first burst after a longer period of quiescence. As Fig. 1 shows, the reaction flow proceeds along the tin isotopic chain via a sequence of $\beta$ decays of tin isotopes and subsequent proton

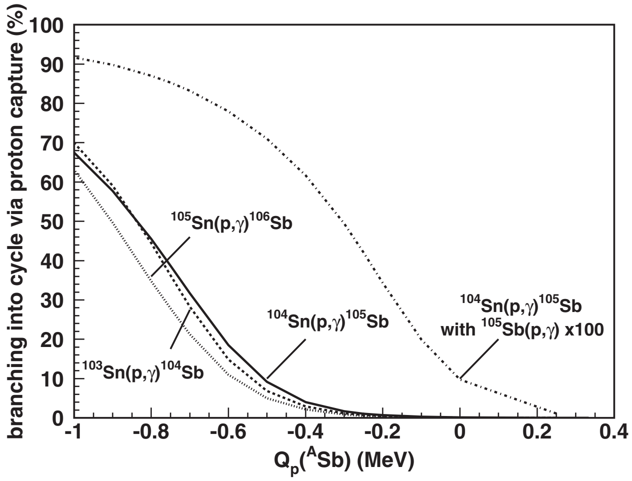


FIG. 4. The branching of the $rp$-process reaction flow into net proton capture and therefore into a Sn-Sb-Te cycle at various tin isotopes as a function of $Q_p = -Q_{(p,\gamma)}$, where $Q_{(p,\gamma)}$ is the $Q$ value for proton capture on the respective tin isotope. The dash-dotted line shows the result for $^{104}$Sn when the $^{105}$Sb$(p, \gamma)$ reaction rate is increased by a factor of 100.

capture on the indium daughters. Net proton capture on the very neutron deficient tin isotopes is prevented by fast $(\gamma, p)$ photodisintegration on the corresponding antimony isotone owing to large $Q_p$ values. As the reaction flow proceeds towards stability it reaches a point where $Q_p$ of the antimony isotopes becomes small enough for net proton capture to become efficient. This occurs at $^{105}$Sn, where a significant fraction of the reaction flow branches into a proton-capture path and therefore into a Sn-Sb-Te cycle.

Of particular interest here is the question of whether the new constraints on $S_p$ values for $^{104}$Sb and $^{105}$Sb allow the establishment of Sn-Sb-Te cycle at $^{104}$Sn or even at $^{103}$Sn. All the tellurium isotopes in this region are $\alpha$ unbound and therefore a cycle will be established whenever the proton-capture reaction sequence reaches tellurium. The branching into proton-capture flow at $^{103}$Sn and $^{104}$Sn predicted by the x-ray burst model for a sequence of $Q_p$ values for $^{104}$Sb and $^{105}$Sb are shown in Fig. 4. Clearly, $Q_p$ values of less than $-500$ keV would be needed in all cases for a significant Sn-Sb-Te cycle to be established.

In principle, the proton-capture flow branching at the tin isotopes represents a $2p$ capture sequence [22] and therefore depends on the proton-capture rate of the resulting antimony isotones. This proton capture depletes the abundance in the $(p, \gamma)$-$(\gamma, p)$ equilibrium system established between the tin and the weakly bound or unbound antimony isotones. Therefore, a larger $^{A}$Sb$(p, \gamma)$ rate would increase the net proton-capture branch at a given $^{A-1}$Sn isotope. For the case of $^{104}$Sn, Fig. 4 shows that for an extreme increase of the $^{105}$Sb$(p, \gamma)^{106}$Te reaction rate by a factor of 100, the maximum $Q_p$ for $^{105}$Sb to establish a significant Sn-Sb-Te cycle at $^{104}$Sn would require $Q_p = 0$. With the new data for $^{105}$Sb this can now be excluded with certainty.

Our estimate of the lowering of $Q_p(^{104}$Sb) following from the pairing effects in the iodine isotopes would need to be extremely large for the Sn-Sb-Te cycle to form at $^{103}$Sn. Therefore, it appears more likely that the cycle develops at $^{105}$Sn. This is illustrated in Fig. 4.

With the published experimental value of $Q_p = -930 \pm 210$ keV for $^{106}$Sb [32], a strong cycle would be established, though very late in the burst. However, this value is questionable [18] and with the recommended $Q_p$ value of $-680$ to $-40$ keV for $^{106}$Sb, the branching into the Sn-Sb-Te cycle at $^{105}$Sn would be significantly reduced and could essentially be zero. A new mass measurement of $^{106}$Sb would clarify this issue.

In summary, the very small $\alpha$-decay branch of $^{109}$I, $b_\alpha = (1.4 \pm 0.4) \times 10^{-4}$, has been observed for the first time. The $Q_\alpha(^{109}$I) value of $3918 \pm 21$ keV allowed the indirect measurement of $Q_p(^{105}$Sb$) = 356 \pm 22$ keV, which is about 130 keV lower than previously claimed. This difference increases the partial half-life for proton decay by several orders of magnitude, making the probability of observing direct proton decay of $^{105}$Sb very small, much below any previously-set experimental limit. The new $Q_p$ value of $^{105}$Sb excludes the formation of a Sn-Sb-Te cycle at $^{104}$Sn and the corresponding enhancement in energy production and x-ray luminosity during the tail end of an x-ray burst. However, with our new estimated $Q_p$ value for $^{104}$Sb such an enhancement becomes a possibility through the formation of a cycle at $^{103}$Sn if the $^{104}$Sb$(p, \gamma)^{105}$Te reaction rate is strongly underestimated.

This work was supported in part by the US DOE under Grants No. DE-AC05-060R23100, No. DE-FG02-96ER40983, No. DE-AC05-00OR22725, No. DE-FG02-96ER-41006, No. DE-FG05-88ER40407, the UNIRIB consortium, the UK EPSRC, and the Foundation for Polish Science. H. S. is supported by NSF Grants No. PHY 0606077 and No. PHY 0216783 (JINA).

[1] E. Rutherford, Philos. Mag. **47**, 109 (1899).
[2] K. P. Jackson *et al.*, Phys. Lett. **33B**, 281 (1970).
[3] E. Roeckl, Radiochimica Acta **70/71**, 107 (1995).
[4] M. Karny *et al.*, Phys. Rev. Lett. **90**, 012502 (2003).
[5] S. N. Liddick *et al.*, Phys. Rev. Lett. **97**, 082501 (2006).
[6] R. D. Page *et al.*, Phys. Rev. C **49**, 3312 (1994).
[7] R. Kirchner *et al.*, Phys. Lett. **70B**, 150 (1977).
[8] E. Roeckl *et al.*, Z. Phys. A **294**, 221 (1980).
[9] T. Faestermann *et al.*, Phys. Lett. **137B**, 23 (1984).
[10] R. D. Page *et al.*, Phys. Rev. Lett. **72**, 1798 (1994).
[11] R. Tighe *et al.*, Phys. Rev. C **49**, R2871 (1994).
[12] M. Shibata *et al.*, Phys. Rev. C **55**, 1715 (1997).
[13] Z. Liu *et al.*, Phys. Rev. C **72**, 047301 (2005).
[14] G. Berthes, GSI Report No. GSI-87-12, 1987, p. 80–89.
[15] J. Friese, *Proceedings of the XXIV Hirschegg Workshop* (GSI Report ISSN 0720-8715, 1996), p. 123.
[16] K. Rykaczewski *et al.*, Phys. Rev. C **52**, R2310 (1995).
[17] A. Gillitzer *et al.*, Z. Phys. A **326**, 107 (1987).
[18] G. Audi *et al.*, Nucl. Phys. **A729**, 337 (2003).

[19] P. J. Sellin *et al.*, Phys. Rev. C **47**, 1933 (1993).
[20] A. Hecht *et al.*, AIP Conf. Proc. **819**, 355 (2006).
[21] R. K. Wallace *et al.*, Astrophys. J. Suppl. Ser. **45**, 389 (1981).
[22] H. Schatz *et al.*, Phys. Rep. **294**, 167 (1998).
[23] S. Woosley *et al.*, Astrophys. J. Suppl. Ser. **151**, 75 (2004).
[24] H. Schatz *et al.*, Phys. Rev. Lett. **86**, 3471 (2001).
[25] C. J. Gross *et al.*, Nucl. Instrum. Methods Phys. Res., Sect. A **450**, 12 (2000).
[26] D. Shapira *et al.*, Nucl. Instrum. Methods Phys. Res., Sect. A **454**, 409 (2000).
[27] M. N. Tantawy *et al.*, Phys. Rev. C **73**, 024316 (2006).
[28] R. Grzywacz, Nucl. Instrum. Methods Phys. Res., Sect. B **204**, 649 (2003).
[29] S. Hofmann, in *Nuclear Decay Modes*, edited by D. N. Poenaru (IOP Publishing, London, 1996), p. 143.
[30] F. Heine *et al.*, Z. Phys. A **340**, 225 (1991).
[31] H. Keller *et al.*, Z. Phys. A **340**, 363 (1991).
[32] A. Płochocki *et al.*, Phys. Lett. **106B**, 285 (1981).
[33] D. Schardt *et al.*, Nucl. Phys. **A368**, 153 (1981).